Int. J. Heat Mass Transfer. Vol. 34, No. 10, pp. 2475–2482, 1991
Printed in Great Britain

0017-9310/91 $3.00+0.00
Pergamon Press plc

Numerical simulation of transitional flow and heat transfer in a smooth pipe

ZHU HUIREN and LIU SONGLING
Department of Aeroengine, Northwestern Polytechnical University, Xi'an, Shaanxi 710072, China

(*Received* 11 *September* 1990 *and in final form* 14 *December* 1990)

Abstract—A two-dimensional boundary-layer program STAN5 is modified to incorporate a low-Reynolds number version of the K–ε, two-equation turbulence model to simulate automatically the laminar, transitional and turbulent flow zones and also the onset of transition and to account for the influence of inlet turbulence intensity upon the flow and heat transfer in a smooth pipe. The prediction for Reynolds number ranging from about 1000 to 10000 is made under inlet turbulence intensity ranging from 0.1 to 8.0%. Results show that when $Re < 2068$ and $Re > 4809$, inlet turbulence intensities have no influence upon flow and heat transfer but when $2068 \leqslant Re \leqslant 4809$, the influence is rather strong, and when the inlet turbulence intensity is 1.0%, the predicted relation between average Nusselt number and Reynolds number is in good agreement with the experimental correlation. In the fully developed region, flow and heat transfer are not affected by inlet turbulence intensities, and the agreement between the results and data for the friction coefficient is good.

INTRODUCTION

THE TRANSITIONAL flow and its convective heat transfer in a smooth pipe are areas that have not been fully investigated. Among the early experimental works on transitional heat transfer in a smooth pipe are the contributions by Sherwood and Petrie [1] for the effect of Prandtl number, by Morris and Whitman [2] and Smith [3] for the effect of heating and cooling, and by Sherwood *et al.* [4] for the effect of the pipe length–diameter ratio. The measurements of Cholette [5] give the local and average coefficient of heat transfer for air flow of the laminar, transition and turbulent regions. A fairly detailed study about the effect of high surface-to-fluid temperature ratio, and entrance configuration and pipe length–diameter ratio, etc. has been made by Humble *et al.* [6]. However, among the published experimental data, a great deal of confusion exists for predicting the heat transfer coefficient in the transitional region. One of the main reasons would be that the transition process is very sensible for the turbulence in the flow at the inlet of the pipe. Generally the magnitude of the critical Reynolds number in the pipe flow is 2200, nevertheless it is observed in experiments that if inlet turbulence can be depressed carefully, laminar flow could be maintained to higher Reynolds number [7]. On the contrary, if inlet turbulence increases, transition will take place at a lower Reynolds number [8]. Therefore, in order to simulate transitional flow and heat transfer in a pipe, the effects of inlet turbulence have to be introduced in the calculation model.

In this paper, the boundary layer equation and low-Reynolds number K–ε model are used to study the effect of inlet turbulence intensities on transitional flow and heat transfer in a smooth pipe. The algorithm used to solve convective transport equations is the same as in ref. [9]. A modified version of the Lam–Bremhorst [10] low-Reynolds number turbulence model suggested by the authors, is applied. Calculated results indicate that, using the turbulence model mentioned above, the effect of inlet turbulence intensities on transition and transitional flow can be simulated successfully.

CONVECTIVE TRANSPORT EQUATIONS

The time-mean continuity equation for the pipe flow is given by

$$\frac{\partial}{\partial x}(r\rho U)+\frac{\partial}{\partial r}(r\rho V)=0. \tag{1}$$

The time-mean momentum equation in the x-direction is given by

$$\rho U\frac{\partial U}{\partial x}+\rho V\frac{\partial U}{\partial r}=-\frac{\partial p}{\partial x}+\frac{1}{r}\frac{\partial}{\partial r}\left[r\left(\mu\frac{\partial U}{\partial r}-\rho\overline{uv}\right)\right]. \tag{2}$$

The time-mean stagnation enthalpy equation is given by

$$\rho U\frac{\partial H}{\partial x}+\rho V\frac{\partial H}{\partial r}=\frac{1}{r}\frac{\partial}{\partial r}\left\{r\left[\frac{\mu}{Pr}\frac{\partial H}{\partial r}-\rho\overline{vh'}-\mu\left(1-\frac{1}{Pr}\right)\frac{\partial}{\partial r}\left(\frac{U^2}{2}\right)-\rho U\overline{uv}\right]\right\}. \tag{3}$$

In these equations, the x coordinate coincides with the axis of the pipe; r is normal to and a distance from

NOMENCLATURE

C_μ, C_1, C_2 empirical constants in turbulence model
C_f friction coefficient of fully developed region
C_{fx} local friction coefficient
D pipe diameter
f_μ, f_1, f_2 empirical functions in turbulence model
H mean total enthalpy, $h+U^2/2$
h mean static enthalpy
h' fluctuating static enthalpy
L turbulent length scale
K, ε turbulence kinetic energy and its dissipation rate, respectively
Nu average Nusselt number
Nu_x local Nusselt number
P mean static pressure
Pr molecular Prandtl number
Pr_t turbulent Prandtl number
r distance from axis of pipe
R radius of pipe
Re Reynolds number based on the pipe diameter
Re_y, Re_t turbulence Reynolds number defined in equation (13)
Tu turbulence intensity
U, V time-mean velocity
u, v fluctuating velocity
U_t friction velocity
U^+ non-dimensional velocity, u/U_t
x, X distance in the flow direction from the entrance of the pipe
X^+ non-dimensional distance, $X/(D\,Re\,Pr)$
y, Y distance from the wall, $R-r$
Y^+ non-dimensional distance from the wall
x_0 location of the initial station.

Greek symbols
μ molecular viscosity
μ_t turbulence viscosity defined in equation (11)
ρ density
σ_k, σ_ε empirical constants in the turbulence model.

Subscripts
i inlet station
w wall.

the axis, and the thermodynamic quantity–velocity fluctuation correlations are neglected.

It is assumed that the profiles of velocity and total enthalpy are both symmetric to the axis of the pipe, therefore, the following boundary conditions at the axis can be taken:

$$\frac{\partial U}{\partial r}=0,\quad \frac{\partial H}{\partial r}=0. \tag{4}$$

At the pipe wall, if there is no fluid injection or suction, according to the no-slip condition

$$U_w=0,\quad V_w=0\quad (x\geqslant x_0). \tag{5}$$

Assuming the wall temperature is T_w, the boundary condition for the total enthalpy H at the wall is

$$H_w=C_pT_w\quad (x\geqslant x_0) \tag{6}$$

where x_0 is the location of the initial station (to be discussed later).

The initial station should be located in the vicinity of the entrance of the pipe. Owing to the small thickness, the annular boundary layer at initial station could be considered to be approximate to a flat plate boundary layer, therefore a modified Pohlhausen velocity profile [11] can be used

$$\frac{U}{U_i}=[2\eta-2\eta^2+\eta^4]\left(1-\frac{\delta}{R}\right)+[2\eta-\eta^2]\frac{\delta}{R} \tag{7}$$

$$\eta=\begin{cases}y/\delta & \text{for } y<\delta\\ 1.0 & \text{for } y\geqslant\delta\end{cases} \tag{8}$$

where y is the distance from the pipe, δ the boundary layer thickness which can be predicted like that on a flat plate, and R the radius of the pipe.

The total enthalpy distribution at the initial station is related linearly to the velocity profile as shown in ref. [12]

$$\frac{H}{H_i}=1+\left(\frac{H_i}{H_w}-1\right)\frac{U}{U_i}. \tag{9}$$

The turbulent-shear stress $-\rho\overline{uv}$ and turbulent heat flux $-\rho\overline{vh'}$ in equations (2) and (3), can be related to the mean-velocity gradient and mean-total enthalpy gradient, respectively

$$-\rho\overline{uv}=\mu+\frac{\partial U}{\partial r} \tag{10a}$$

$$-\rho\overline{vh'}=\frac{\mu_t}{Pr_t}\frac{\partial H}{\partial r} \tag{10b}$$

where Pr_t is the turbulent Prandtl number, for the pipe flow, by Hishida *et al.*'s data [13], it is equal approximately to 0.9 when $Y^+>30$ and when $Y^+<30$, and increases reaching 1.6 at $Y^+=10$. A constant value of 0.9 has been taken in this paper for simplicity. μ_t is the turbulent viscosity, which has been

modelled by Lam–Bremhorst's K–ε two-equation model as discussed below.

TURBULENCE MODEL

In order to simulate the transition process, it is assumed that turbulence exists in any real laminar flow, if turbulence increases and reaches a certain extent, laminar flow will become turbulent. If we can model this process by the numerical method, it is possible to predict transition automatically.

It should be noticed that most of the commonly used turbulence models are unsuitable for this circumstance, because the effect of viscosity has not been considered and it is very important for transition.

In 1972, Jones and Launder [14] suggested a low-Reynolds number K–ε turbulence model. The main feature of this model is that the viscosity of fluid is taken into account, therefore it can be used in the vicinity of the wall and would be suitable for simulating transitional flow. In 1981, Lam and Bremhorst [10] modified the model and adjusted the form of some parameters to make it more perfect. Rodi and Scheuerer [12] used the modified model to calculate external boundary layer transition with some success. In this paper the low Reynolds number K–ε model suggested by Lam–Bremhorst is used with some modifications to simulate the transition process in the pipe which has not been seen in published papers before. In the model used in this paper turbulent viscosity can be expressed as

$$\mu_t = C_\mu f_\mu \rho \frac{K^2}{\varepsilon} \tag{11}$$

where C_μ is a constant and f_μ takes the following form:

$$f_\mu = [1-\exp(-0.016Re_y)]^2(1+19.5/Re_t) \tag{12}$$

$$Re_y = \begin{cases} K^{1/2}Y\rho/\mu & (Y < \delta) \\ K^{1/2}\delta\rho/\mu & (Y \geqslant \delta) \end{cases} \tag{13a}$$

$$Re_t = \rho K^2/(\mu\varepsilon). \tag{13b}$$

Both K and ε can be calculated by the following equations:

$$\rho U\frac{\partial K}{\partial x}+\rho V\frac{\partial K}{\partial r} = \frac{1}{r}\frac{\partial}{\partial r}\left[r\left(\mu+\frac{\mu_t}{\sigma_k}\right)\frac{\partial K}{\partial r}\right]+p_k-\rho\varepsilon \tag{14}$$

$$\rho U\frac{\partial \varepsilon}{\partial x}+\rho V\frac{\partial \varepsilon}{\partial r} = \frac{1}{r}\frac{\partial}{\partial r}\left\{r\left[\left(\mu+\frac{\mu_t}{\sigma_\varepsilon}\right)\frac{\partial \varepsilon}{\partial r}\right]\right\} + \frac{\varepsilon}{K}[C_1 f_1 p_k - C_2 f_2 \rho\varepsilon] \tag{15}$$

in which

$$P_k = \rho\left(\frac{\partial U}{\partial r}\right)^2 \tag{16}$$

is the production of turbulence kinetic energy. f_1 and f_2 take the following form:

$$f_1 = 1+\left(\frac{0.06}{f_\mu}\right)^3; \quad f_2 = 1-\exp(-Re_t)^2. \tag{17}$$

The empirical constants in equations (11), (14) and (15) take the following values:

$$C_\mu = 0.09; \quad C_1 = 1.44; \quad C_2 = 1.92; \quad \sigma_k = 1.0; \quad \sigma_\varepsilon = 1.3. \tag{18}$$

The boundary conditions of equations (14) and (15) are

on the axis

$$\frac{\partial K}{\partial r} = \frac{\partial \varepsilon}{\partial r} = 0 \tag{19a}$$

on the wall

$$K = \frac{\partial \varepsilon}{\partial r} = 0. \tag{19b}$$

The initial profiles of turbulent kinetic energy K and its dissipation rate ε play important roles in the calculation. It is assumed that these profiles are composed of two parts. The first part is similar to turbulent flow even though these profiles are taken in the laminar region. According to the classical mixing length theory and equation (11), using the method similar to ref. [15], the expressions for both turbulent kinetic energy and its dissipation can be obtained

$$K = \left(\frac{\partial U}{\partial y}\right)^2 l^2/(C_\mu f_\mu)^{1/2} \tag{20a}$$

$$\varepsilon = (C_\mu f_\mu)^{3/4}K^{3/2}/l \tag{20b}$$

where the mixing length L is determined from the following expressions:

$$L = 0.41y, \quad \text{for } y < 0.09\delta/0.41$$
$$L = 0.09\delta, \quad \text{for } y \geqslant 0.09\delta/0.41$$

where 0.41 is the von Karman constant.

The second part comes from the influence of inlet turbulence intensity. It can be seen from equations (20a) and (20b) that K and ε will take the value of zero at the outer edge of the boundary layer. This is true only in the case of no turbulence intensity in the free stream. If we assume that inlet turbulence intensity produces a linear profile for K and ε then the initial profiles for them will take the following forms:

$$K = \frac{l^2}{(C_\mu f_\mu)^{1/2}}\left(\frac{\partial U}{\partial y}\right)^2 + K_i\eta \tag{21a}$$

$$\varepsilon = [(C_\mu f_\mu)^{3/4}K^{3/2}/l+\varepsilon_i\eta]C_0 \tag{21b}$$

where η is defined in equation (8), C_0 is a constant along the pipe, K_i and ε_i are turbulent kinetic energy

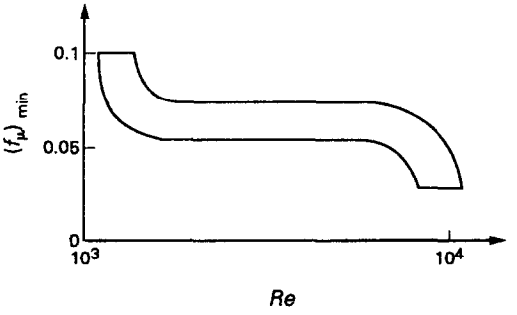

FIG. 1. Relation between $(f_\mu)_{min}$ and Re.

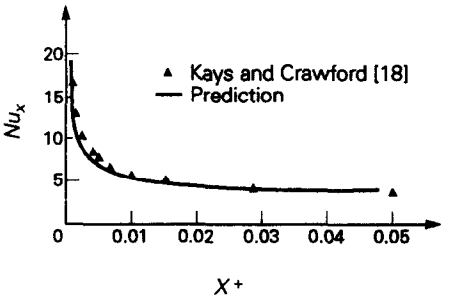

FIG. 3. Comparison of local Nusselt number profiles with the results of Kays and Crawford.

and its dissipation rate in the inlet flow, given, respectively, by

$$K_i = 1.5(U_i Tu_i)^2 \tag{22a}$$

$$\varepsilon_i = (C_\mu f_\mu)^{3/4} K_i^{3/2}/l. \tag{22b}$$

Calculations show that if this turbulence model is used, good results could not be obtained unless the following problems are treated properly:

(1) The initial profile of ε should be set up properly. Up to now, we know very little about the behaviour of ε in the laminar zone. The constant C_0 in equation (21b) is used to adjust the profile. The correlation plotted in Fig. 1 indicates its suggested values, which are related to the Reynolds number Re.

(2) The profile behaviour of f_μ should be set up. The minimum value of f_μ should be limited near the wall. Calculation results show that if f_μ is determined by equation (11) near the wall, it will take too small a value, and a large value of ε will be obtained, which will prevent the transition from taking place. Therefore, the minimum value of f_μ should be limited. Chapman and Kuhn [17] give a different profile of f_μ near the wall from that determined by equation (11). In this paper, we took it as a constant that depends upon the Reynolds number Re as shown in Fig. 2.

It is also discovered that C_0 and $(f_\mu)_{min}$ are both related to inlet turbulence intensity.

RESULTS AND DISCUSSION

The numerical simulation of flow and heat transfer in a pipe is made at constant pipe wall temperature. The Reynolds number Re ranging from 1000 to 10 000, and inlet turbulence intensities Tu_i from 0.1 to 8.0%. The results are discussed below.

(1) Re = 1050–1850

It can be seen from Figs. 3 and 4, that the predicted local Nusselt number and friction coefficient for different inlet turbulence intensity levels are both in good agreement with Kays and Crawford's [18] and Langhaar's [19] results, respectively. This shows that when the Reynolds number is lower than 1850, inlet turbulence intensities do not affect significantly the local Nusselt number and the friction coefficient. In these cases inlet turbulent fluctuation decays along with the motion of the fluid. Figure 5 presents calculated turbulence kinetic energy profiles on eleven sections along the pipe. From $X^+ = 0.00034$ to 0.0009, turbulence kinetic energy decreases rapidly, after that it decreases gradually and approaches zero at about $X^+ = 0.027$. It can be seen that the decay is moving from the wall to the centre of the pipe.

(2) Re = 2068–4490

In Fig. 6 the predicted local Nusselt number Nu_x is given for the case of a Reynolds number of 2068. When inlet turbulence intensities vary from 0.1 to 1.0%, the flow in the pipe stays laminar. When inlet

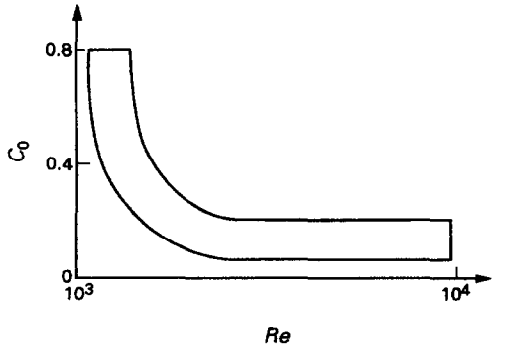

FIG. 2. Relation between C_0 and Re.

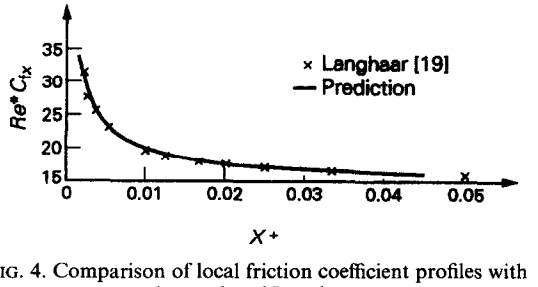

FIG. 4. Comparison of local friction coefficient profiles with the results of Langhaar.

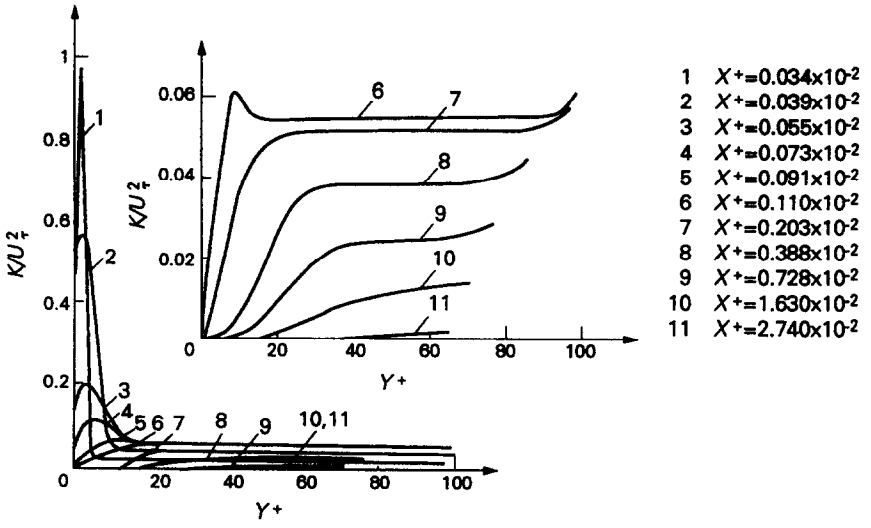

FIG. 5. Turbulent kinetic energy distribution at different sections along the pipe.

turbulence intensity is raised to 3.0% or higher, there is a rapid increase in the local Nusselt number which can be considered as an indication of transition from laminar to turbulent flow taking place. The higher the inlet turbulence intensity, the earlier transition occurs. After completing the transition the local Nusselt number has nearly the same value for different inlet turbulence intensities. This means that the magnitude of inlet turbulence only affects the transition and does not give an important influence on the fully developed turbulent flow. This seems to be different from the case of external flow for which free stream turbulence has an influence upon the turbulent boundary layer [20, 21].

When the Reynolds number is equal to 2302–4990, similar results can be obtained, and in these cases transition is always present even though the inlet turbulence intensity takes a rather small value (0.1%).

(3) $Re = 4809$–9200

In Figs. 7 and 8 the predicted local Nusselt number and local friction coefficient are given for three inlet turbulence intensities with $Re = 4809$. It can be seen that these curves have small differences in the transitional zone, which means that inlet turbulence intensity has a rather weak effect on the flow of this case. Similar results have been obtained at higher Reynolds numbers, however, the difference in the transitional zone became smaller than that given in Figs. 7 and 8.

(4) The predicted average Nusselt number for

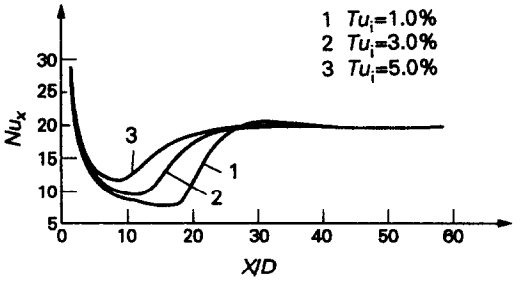

FIG. 7. Local Nusselt number distribution of $Re = 4809$.

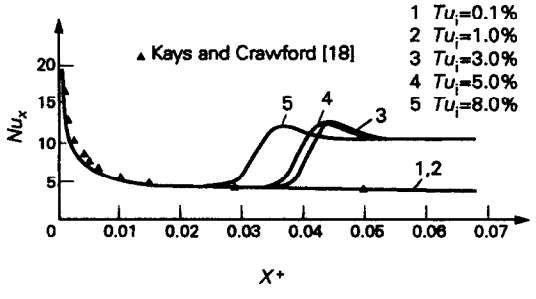

FIG. 6. Local Nusselt number distribution of $Re = 2068$.

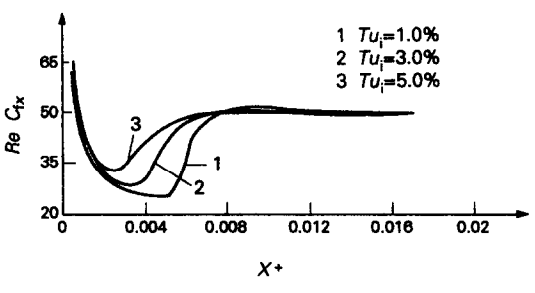

FIG. 8. Local friction coefficient distribution of $Re = 4809$.

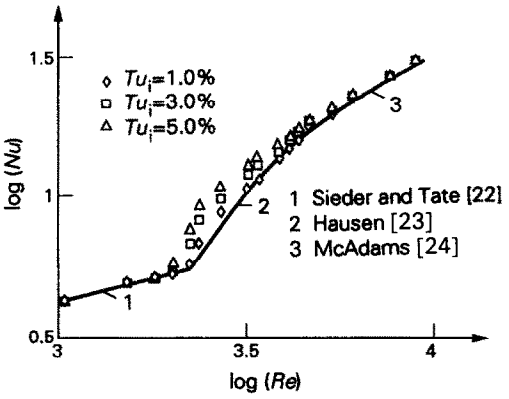

FIG. 9. Comparison of average Nusselt number results with the commonly used formula.

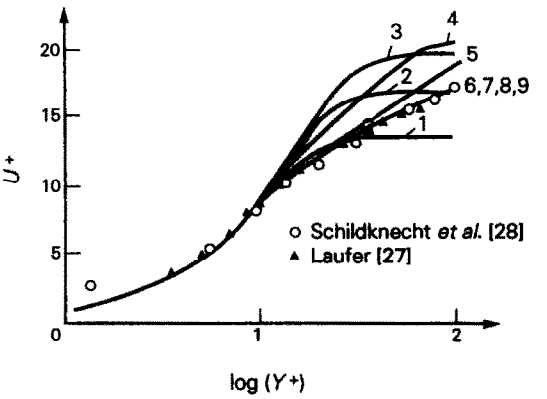

FIG. 11. Velocity distribution at different sections along the pipe.

different Reynolds number and inlet turbulence intensities are shown in Fig. 9. If $Re < 2068$ Nu does not relate to inlet turbulence intensities, and agrees with the well-known laminar formula [22]. When $2068 \leqslant Re \leqslant 4809$, average Nusselt numbers vary with Tu_i, the predicted relation between Nu and Re at $Tu_i = 1.0\%$ is in good agreement with that given in ref. [23]. When $Re > 4809$, Nu does not relate to inlet turbulence intensities, and agrees with the commonly used turbulent flow formula [24, 25].

The friction coefficient of the fully developed region is given in Fig. 10 only for $Tu_i = 3.0\%$. The inlet turbulence intensities have a very weak influence on the friction coefficient in this region (see Fig. 8). The predicted value is in good agreement with that introduced in ref. [26].

In order to study the whole process of transition, the profiles of velocity, turbulence kinetic energy and its dissipation rate on nine sections along the pipe are given in Figs. 11–13 at a Reynolds number of 4809 and an inlet turbulence intensity of 8.0%. The locations of these sections are listed in Table 1.

It can be seen from Fig. 7 or Fig. 8 that sections 1–3 are located in the laminar region; sections 4 and 5 are transitional and sections 6–9 are fully developed flow.

The velocity profiles for these sections are given in Fig. 11. The modified Pehlhausen profile is assumed as the initial condition in the calculation. In sections 6–9, the profiles become invariable and agree excellently with the measurement for the fully developed turbulent profile given in refs. [27, 28].

The turbulence kinetic energy of these sections is plotted in Fig. 12. From sections 1 to 2, turbulence kinetic energy decreases moderately, from sections 2 to 3, it still decreases in the outer part of the boundary layer and increases in the inner part. From sections 3 to 4 and to 5 turbulence kinetic energy K increases rapidly, which comes from the unbalance between the production term and dissipation term in equation (14), therefore the transition to turbulence takes place. In this process, the set of maximum turbulence kinetic

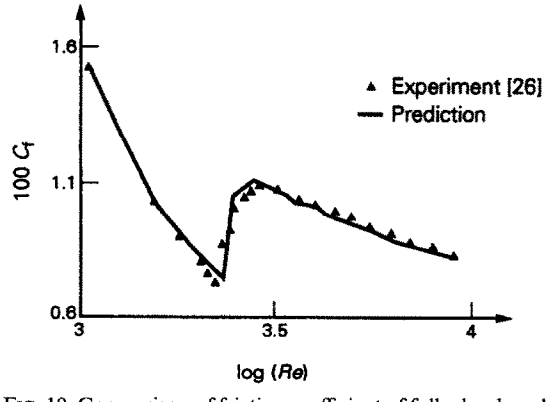

FIG. 10. Comparison of friction coefficient of fully developed region with the experimental data.

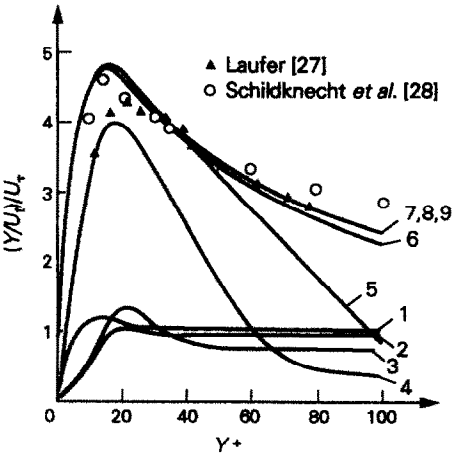

FIG. 12. Turbulent kinetic energy distribution at different sections along the pipe.

Table 1

	Number								
	1	2	3	4	5	6	7	8	9
$100X^+$	0.05	0.09	0.15	0.34	0.46	0.93	1.23	1.53	1.84
X/D	1.79	3.29	5.80	12.06	16.10	32.55	43.08	53.79	64.69

energy is moving to the wall gradually. The profiles of sections 7–9 are nearly the same. The agreement of these profiles with the measured data given in refs. [27, 28] is good. It is noticed that the site of largest turbulence kinetic energy is located at about $Y^+ = 10$–30. This is the value corresponding to the outer edge of the buffer layer of turbulent flow.

In Fig. 13, the turbulent kinetic energy dissipation rate of these sections are plotted. In the fully developed region, agreement between prediction and data [27] is good.

CONCLUSIONS

From the predication results given in this paper the following conclusions can be drawn:

(1) When $Re < 1850$, the transition from laminar to turbulence will not be present even if the inlet turbulence intensity is rather large ($Tu_i = 8.0\%$).

(2) When $Re < 2068$ and $Re > 4809$, inlet turbulence intensities have no significant influence on average Nusselt number in the long pipe ($X/D = 60$).

(3) When $2068 \leqslant Re \leqslant 4809$, the average Nusselt number of the long pipe is influenced by the inlet turbulence intensities. The predicted results under $Tu_i = 1.0\%$ are in good agreement with the relation introduced in ref. [23].

(4) The fully developed region does not influence the inlet turbulence intensity and for the friction coefficient of this region, the agreement between the predicted value and experimental data introduced in ref. [26] is good.

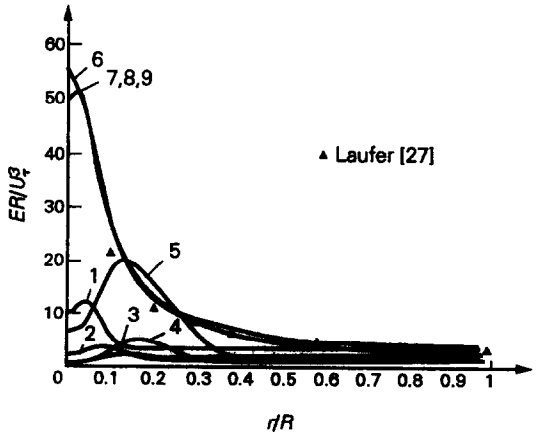

FIG. 13. Distribution of turbulent kinetic energy dissipation at different sections along the pipe.

REFERENCES

1. T. K. Sherwood and J. M. Petrie, Heat transmission to liquids flowing in pipes, *Ind. Engng Chem.* **24,** 736–745 (1932).
2. F. H. Morris and W. G. Whitman, Heat transfer for oils and water in pipes, *Ind. Engng Chem.* **20,** 234–240 (1928).
3. J. F. D. Smith, Heat transfer and pressure drop data for an oil in a copper tube, *Trans. Am. Inst. Chem. Engrs* **31,** 83–112 (1935).
4. T. K. Sherwood, D. D. Kiley and G. E. Mangsen, Heat transmission to oil flowing in pipes effect of tube length, *Ind. Engng Chem.* **24,** 273–277 (1932).
5. A. Cholette, Local and average coefficients for air flowing inside tubes, *Chem. Engng Prog.* **44**(1), 81–88 (1948).
6. L. V. Humble, H. W. Lowdermilk and L. L. Desmon, Measurements of average heat-transfer and friction coefficients for subsonic flow of air in smooth tubes at high surface and fluid temperatures, NACA Report 1020 (1951).
7. W. Pfenniger, *Boundary Layer and Flow Control.* Pergamon Press, Oxford (1961).
8. D. J. Tritton, *Physical Fluid Dynamics.* Van Nostrand Reinhold (1977).
9. M. E. Crawford and W. M. Kays. STAN5—a program for numerical computation of two-dimensional internal external boundary layer flows, NASA CR-2742 (1976).
10. C. K. G. Lam and K. Bremhorst, A modified form of the *K–E* model for predicting wall turbulence, *Trans. ASME* **103,** 1308–1319 (September 1981).
11. A. H. Shapiro, R. Siegel and S. J. Kleine, Friction factor in laminar entry region of a smooth tube, *Proc. 2nd U.S. Natn. Congress of Applied Mechanics*, pp. 733–741 (1954).
12. W. Rodi and G. Scheuerer, Calculation of heat transfer to convection-cooled gas turbine blades, *Trans. ASME* **107,** 620–627 (July 1985).
13. M. Hishida, Y. Nagano and M. Tagawa, Transport processes of heat and momentum in the wall region, *Proc. Eighth Int. Heat Transfer Conf.*, Vol. 3, pp. 925–930 (1986).
14. W. P. Jones and B. E. Launder, The prediction of laminarization with a two-equation model of turbulence, *Int. J. Heat Mass Transfer* **15,** 301–314 (1972).
15. H. Ozoe, A. Mouri, M. Hiramitsu, S. W. Churchill and N. Lior, Numerical calculation of three-dimensional turbulent natural convection in an enclosure using a two-equation model. In *Fundamentals of Natural Convection/Electronic Equipment Cooling*, ASME HTD, Vol. 32, pp. 25–32 (1984).
16. J. H. Wang, H. F. Jen and E. O. Hartol, Airfoil heat transfer calculation using a low Reynolds number version of two-equation turbulence model, *J. Engng Gas Turbine Pwr* **107,** 60–66 (January 1985).
17. D. R. Chapman and G. D. Kuhn, The limiting behaviour of turbulence near a wall, *J. Fluid Mech.* **170,** 265–292 (1986).

18. W. M. Kays and M. E. Crawford, *Convective Heat and Mass Transfer*, 2nd Edn. McGraw-Hill, New York (1980).
19. H. L. Langhaar, Steady flow in the transition length of a straight tube, *J. Appl. Mech.* **9**, A55-58 (June 1942).
20. M. F. Elair, Influence of free-stream turbulence on turbulent boundary-layer heat transfer and mean profile development, part 1—experimental data, *ASME J. Heat Transfer* **105**, 33–40 (1983).
21. J. C. Simonich and P. Bradshaw, Effect of free-stream turbulence on heat transfer through a turbulent boundary layer, *ASME J. Heat Transfer* **100**, 671–677 (November 1978).
22. E. N. Sieder and G. E. Tate, Heat transfer and pressure drop of liquids in tubes, *Ind. Engng Chem.* **28**, 1429–1435 (1936).
23. H. Hausen, Darstellung des Wärmeuberganges in Rohren durch Verallgemeinerte Potenzbeziehungen, *VDIZ* No. 4, 91–98 (1943).
24. W. H. McAdams, Review and summary of developments in heat transfer by conduction and convection, *Trans. A.I.Ch.E.* **36**, 1–20 (1940).
25. W. M. Kays and H. C. Perkins, *Handbook of Heat Transfer* (Edited by W. M. Rohsenow and J. P. Hartnett), Chap. 7. McGraw-Hill, New York (1972).
26. D. H. Schlichting, *Boundary-layer Theory*, 7th Edn. McGraw-Hill, New York (1987).
27. J. Laufer, The structure of turbulence in fully developed pipe flow, NACA Rept. 1174 (1954).
28. M. Schildknecht, J. A. Miller and G. E. A. Meier, The influence of suction on the structure of turbulence in fully developed pipe flow, *J. Fluid Mech.* **90**, 67–107 (January 1979).

SIMULATION NUMERIQUE DE L'ECOULEMENT DE TRANSITION ET DE TRANSFERT THERMIQUE DANS UN TUBE LISSE

Résumé—Un programme STAN5 à couche limite bidimensionnelle est modifié pour introduire une version K–ε à faible nombre de Reynolds pour simuler automatiquement les zones d'écoulement laminaire, transitionnel et turbulent et aussi l'apparition de la transition et pour tenir compte de l'influence de l'intensité de turbulence à l'entrée sur l'écoulement et le transfert thermique dans le tube. La prédiction pour un nombre de Reynolds variant de 1000 à 10 000 concerne une intensité de turbulence à l'entrée allant de 0,1 à 8,0%. Les résultats montrent que lorsque $Re < 2068$ et $Re > 4809$, les intensités de turbulence n'ont pas d'influence sur l'écoulement et le transfert thermique; mais lorsque $2068 \leqslant Re \leqslant 4809$, l'influence est forte et quand l'intensité de turbulence est 1%, la relation prédite entre le nombre de Nusselt moyen et le nombre de Reynolds s'accorde bien avec la formulation expérimentale. Dans la région pleinement établie, l'écoulement et le transfert thermique ne sont pas affectés par les intensités de turbulence à l'entrée et l'accord entre les résultats du calcul et les données expérimentales pour le coefficient de frottement est bon.

NUMERISCHE SIMULATION DER STRÖMUNG UND DES WÄRMEÜBERGANGS IN EINEM GLATTEN ROHR IM ÜBERGANGSBEREICH

Zusammenfassung—Ein vorhandenes Program (STAN5) zur Berechnung zweidimensionaler Grenzschichtströmungen wird durch Einführen eines K–ε-Zweigleichungs-Turbulenzmodells für kleine Reynolds-Zahlen erweitert. Damit kann es automatisch die Strömung im laminaren, im Übergangs- und im turbulenten Bereich sowie das Einsetzen des Übergangs simulieren. Außerdem wird der Einfluß der anfänglichen Turbulenzintensität auf Strömung und Wärmeübergang in einem glatten Rohr berücksichtigt. Es werden Berechnungen für Reynolds-Zahlen im Bereich von 1000 bis 10 000 und für anfängliche Turbulenzintensitäten von 0,1–8,0% durchgeführt. Es zeigt sich, daß für $Re < 2068$ und $Re > 4809$ die anfängliche Turbulenzintensität keinen Einfluß auf Strömung und Wärmeübergang ausübt, und daß dieser Einfluß im Bereich $2068 \leqslant Re \leqslant 4809$ recht stark ist. Für den Fall einer anfänglichen Turbulenzintensität von 1,0% stimmt die Abhängigkeit der berechneten Nusselt-Zahl von der Reynolds-Zahl gut mit der Korrelation von Versuchsdaten überein. Im Bereich der voll ausgebildeten Strömung verschwindet der Einfluß der anfänglichen Turbulenzintensität auf Strömung und Wärmeübergang vollständig. Die Übereinstimmung zwischen Rechenergebnissen und vorhandenen Daten für den Reibungsbeiwert ist in diesem Bereich gut.

ЧИСЛЕННОЕ МОДЕЛИРОВАНИЕ НЕСТАЦИОНАРНОГО ТЕЧЕНИЯ И ТЕПЛОПЕРЕНОСА В ГЛАДКОЙ ТРУБЕ

Аннотация—Программа STAN5 для двумерного пограничного слоя модифицируется для учета двухпараметрической K–ε модели турбулентности в случае низких чисел Рейнольдса с целью автоматического моделирования ламинарного, нестационарного и турбулентного течений, а также возникновения переходного состояния и с целью определения влияния интенсивности турбулентности на входе на течение и теплоперенос в гладкой трубе. Числа Рейнольдса изменяются в диапазоне от 1000 до 10 000 при изменении интенсивности турбулентности на входе от 0,1 до 8,0%. Полученные результаты показывают, что при числах Рейнольдса $Re < 2068$ и $Re > 4809$ интенсивность турбулентности на входе не оказывает влияния на течение и теплоперенос, в то время как при $2068 \leq Re \leq 4809$ ее влияние довольно существенно. При значении интенсивности турбулентности на входе, составляющем 1,0%, полученное соотношение между средними числами Нуссельта и Рейнольдса хорошо согласуется с экспериментально установленным. В полностью развитой области течение и теплоперенос не зависят от интенсивности турбулентности на входе и расчетные результаты для коэффициента трения хорошо согласуются с экспериментальными данными.